Materials Transactions, Vol. 46, No. 10 (2005) pp. 2246 to 2252
©2005 The Japan Institute of Metals

Preparation of Calcium Phosphate Films by Radiofrequency Magnetron Sputtering

Takayuki Narushima[1], Kyosuke Ueda[2,*], Takashi Goto[3], Hiroshi Masumoto[3], Tomoyuki Katsube[1], Hiroshi Kawamura[4], Chiaki Ouchi[2] and Yasutaka Iguchi[2]

[1]*Tohoku University Biomedical Engineering Research Organization (TUBERO), Sendai 980-8579, Japan*
[2]*Department of Materials Processing, Tohoku University, Sendai 980-8579, Japan*
[3]*Institute for Materials Research, Tohoku University, Sendai 980-8577, Japan*
[4]*Graduate School of Dentistry, Tohoku University, Sendai 980-8575, Japan*

Calcium phosphate films were prepared on titanium substrates by radiofrequency (RF) magnetron sputtering at RF powers from 75 to 150 W. Hot-pressed β-tricalcium phosphate (β-TCP) plates with a high density (>99.6%) were used as a sputtering target. The substrate was not intentionally heated. The films consisted of amorphous calcium phosphate and oxyapatite ($Ca_{10}(PO_4)_6O$) phases. The ratio of the oxyapatite phase depended on the sputtering conditions of RF power, oxygen gas concentration in the sputtering gas (C_{O_2}) and total pressure in the chamber. The (002) preferred orientation of oxyapatite phase was observed. The deposition rate of films increased with increasing RF power and decreasing C_{O_2}. The highest deposition rate was 0.143 nm·s^{-1} (0.515 μm·h^{-1}).

(Received May 20, 2005; Accepted August 17, 2005; Published October 15, 2005)

Keywords: *calcium phosphate, oxyapatite, sputtering, biomaterials, titanium*

1. Introduction

Calcium phosphates such as hydroxyapatite ($Ca_{10}(PO_4)_6(OH)_2$, HAp) and tricalcium phosphate ($Ca_3(PO_4)_2$, TCP) have been used as ceramic biomaterials[1)] with osteoconductivity[2–6)] and bioresorbability.[7–10)] One of their applications is coating for metallic implants. Many experimental deposition processes have been investigated, including plasma spraying, sputtering, pulsed laser deposition, dip coating, sol–gel and electrophoretic deposition.[11)] Among these processes, the plasma spraying[12–21)] has advantages of high deposition rates with sufficiently low cost, and then, titanium dental implants are widely coated with HAp by using plasma spraying.[22)] The plasma-sprayed calcium phosphate coatings, however, show poor adherence to the metal substrate and nonuniformity which limits a critical thickness to ensure complete coverage.

PVD (physical vapor deposition) can be a suitable technique to obtain uniform and dense coatings of calcium phosphates for metal substrates.[23–52)] Radiofrequency (RF) magnetron sputtering has been used in wide areas for coatings of thin films with excellent adherence to substrates,[43)] and applied to coatings of calcium phosphate films on commercially pure titanium (CP–Ti)[23,37,38,40,44)] and $\alpha + \beta$ type titanium alloys.[33,35,36,41,42,45,47–50)] Ti and its alloys are known as biocompatible metals because of their low elastic modulus, high corrosion resistance and the appropriate combination of strength and ductility. Low processing temperature is also an advantage of RF magnetron sputtering for calcium phosphate coatings for Ti substrates because the mechanical properties of the substrates will be degraded by high processing temperatures.

Plasma-sprayed HAp targets have been commonly used in sputtering for calcium phosphate coatings.[23,33,36,37,40,42)] Sintered HAp targets (relative density $> 95\%$) were used by Lo *et al.*[47)] for calcium phosphate coatings in RF magnetron sputtering and pulsed laser deposition. Zeng *et al.*[52)] reported that the surface roughness of the coatings depended on the density of the sintered HAp targets in the range of the relative density between 65 and 90%. Besides HAp targets, Yamashita *et al.*[39)] used targets in a $CaO–P_2O_5$ glass system for calcium phosphate coatings by RF magnetron sputtering. However, no other materials have been applied as the target for RF magnetron sputtering.

The composition and density of the target material should be well controlled in sputtering to obtain highly adhered coatings, particularly for calcium phosphate coatings. In the present work, therefore, calcium phosphate films were prepared on CP–Ti substrates by RF magnetron sputtering using fully-dense hot-pressed β-TCP targets, and the effects of the process conditions on phases in the films, preferential crystallographic orientation and deposition rates were investigated.

2. Experimental

Calcium phosphate films were prepared on CP–Ti substrates (JIS Grade 2) by RF magnetron sputtering (MS-320, Universal Systems Co., Ltd.) using β-TCP targets. The size of the substrate was 10 mm × 10 mm × 1 mm. The substrate was finally polished with an Al_2O_3 paste (0.3 μm) and then ultrasonically cleaned in acetone for 600 s. The average roughness of the substrate was less than 0.05 μm. β-TCP powder (βTCP-100, Taihei Chemical Industrial Co., Ltd.) was hot-pressed at 1273 K and 20 MPa for 7.2 ks in an argon atmosphere. Before hot-pressing, β-TCP powder was ground in an agate mortar to less than 4 μm in average diameter. The size of the target plate was 51 mm in diameter and 3 mm in thickness. The relative density of the target was more than 99.6%. The target plate was brazed to a Cu backing plate using an indium foil (0.1 mm in thickness and 99.99% pure, Nilaco) at 523 K in air for 1.8 ks.

The sputtering chamber was evacuated to a total pressure less than 5×10^{-4} Pa, and then sputtering gas ($Ar–O_2$

---

[*] Graduate Student, Tohoku University

Table 1 Deposition conditions.

RF power	75–150 W
Distance between target and substrate	45 mm
Total pressure	0.1–15 Pa
Gas flow rate	3.3×10^{-7} $m^3 \cdot s^{-1}$
Sputtering gas	Ar–O_2 (C_{O_2}: 0–95%)
Substrate	CP–Ti (Grade 2) plate
Substrate temperature	<423 K
Target	hot-pressed β-TCP plate (relative density > 99.6%)

mixture gas) was introduced into the chamber. The target was pre-sputtered for 1.2 ks before coating. The total gas flow rate was kept at a value of 3.3×10^{-7} $m^3 \cdot s^{-1}$ and the oxygen gas concentration in the sputtering gas (C_{O_2}) was controlled between 0 and 95% by adjusting the mixing ratio of Ar to O_2 gas. The total pressure in the chamber was varied from 0.1 to 15 Pa, and RF power was changed from 75 to 150 W. The substrate was not intentionally heated, but the substrate temperature was slightly increased during sputtering at most about 423 K. Table 1 summarizes the deposition conditions.

The thickness of the film was measured by profilometry (Alpha-step, KLA Tencor). The phase of the films was identified by X-ray diffraction (XRD) with a low incident angle (α-2θ XRD, $\alpha = 1°$). The crystal orientation of the films was evaluated by θ–2θ XRD. The infrared spectra of the films were measured by a reflection mode Fourier transform infrared (FTIR) spectroscopy (FT/IR-460Plus, JASCO). The contents of Ca and P in the films were determined by fluorescent X-ray spectroscopy (FXS, model920, Kevex) and inductively coupled plasma atomic emission spectroscopy (ICP-AES, ICPS8100, Shimadzu).

3. Results and Discussion

3.1 Target composition

Figure 1 shows α-2θ XRD patterns of the surface of β-TCP targets before and after sputtering for 630 ks compared with that of the source β-TCP powder. All the reflections from the target after sputtering for 630 ks were indexed to β-TCP structure. The ICP analysis for "annular race track"[45] of the target surface revealed that the composition, Ca/P molar ratio, was almost the same as that before sputtering. Boyd *et al.*[45] applied hydroxyapatite (HAp) targets pressed at 10 MPa for 7.2 ks using a pressure filtration die assembly in RF magnetron sputtering. They indicated that the HAp degraded during sputtering with becoming hydroxyl ion deficient forming other calcium phosphate phases and $Ca(OH)_2$ accompanying an increase in Ca/P ratio. Ozeki *et al.*[43] reported the decomposition of HAp changing to α-TCP, β-TCP and CaO during sputtering when unsintered HAp powder was used as a target material. In the present work, however, the degradation of the target was not detected by low-incident angle XRD and ICP-AES. The increase in target density could be effective to avoid the increase in surface temperature during sputtering, resulting in insignificant change of phase and composition of the target surface.

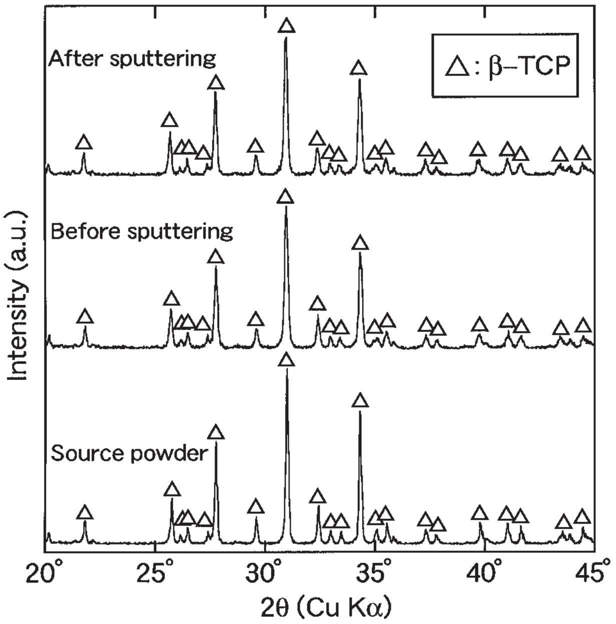

Fig. 1 XRD patterns of β-TCP source powder, and the surface of hot-pressed β-TCP target before and after sputtering for 630 ks.

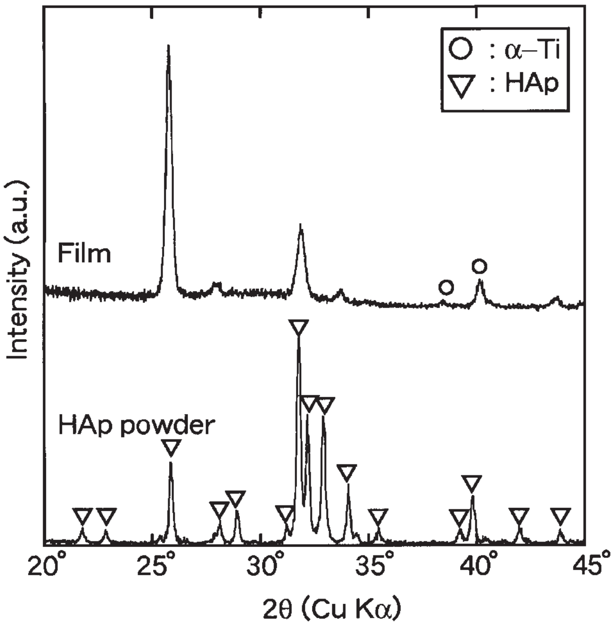

Fig. 2 XRD patterns of film on a CP–Ti substrate and HAp powder as a reference. ($C_{O_2} = 0\%$, RF power = 150 W, total pressure = 0.5 Pa, deposition time = 18 ks)

3.2 Phase and composition of films

Figure 2 shows α-2θ XRD patterns of the film prepared at C_{O_2} of 0%, RF power of 150 W and total pressure of 0.5 Pa for the deposition time of 18 ks. The XRD pattern of HAp powder prepared by grounding a HAp body sintered at 1073 K in air was depicted as comparison. The XRD pattern of the film except the reflections assigned to CP–Ti substrate was almost the same as that of HAp powder. Figure 3 demonstrates the FTIR spectra of the film of Fig. 2 and HAp powder. These spectra were measured by reflection and transmission modes, respectively. A hydroxyl (OH^-) stretch-

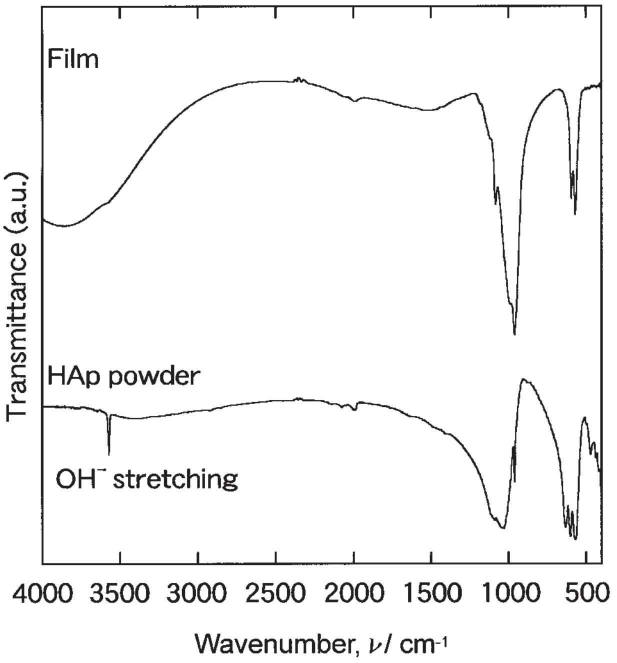

Fig. 3 FTIR spectra of film and HAp powder.

ing band was observed at $3570\,\mathrm{cm^{-1}}$ in the HAp powder, while no $\mathrm{OH^-}$ band was detected in the film. It is known that HAp ($\mathrm{Ca_{10}(PO_4)_6(OH)_2}$) would lose hydroxyl ions and transform to oxyhydroxyapatite (OHAp, $\mathrm{Ca_{10}(PO_4)_6(OH)_{2-2x}O_x\square_x}$, $\square$: vacancy, $X < 1$) or oxyapatite (OAp, $\mathrm{Ca_{10}(PO_4)_6O\square}$) at high temperatures.[53–56] The XRD patterns of these apatites are almost identical.[57] The coating film obtained in the present work could contain the OAp phase because of the similar XRD pattern to HAp and the lack of hydroxyl bands in FTIR spectra. Since the β-TCP target contained no hydroxyl group, the OAp phase might be formed in the films. It has been reported that no hydroxyl bands in FTIR spectra were detected in as-sputtered amorphous calcium phosphate film by RF magnetron sputtering using an HAp target.[23,36,40,44]

Gross *et al.*[57,58] reported the formation of OAp phase after crystallization of plasma-sprayed calcium phosphate film, and the OAp and HAp phases could be identified using the (00*l*) peaks in XRD patterns. In the present work, however, no shift and separation of (00*l*) peaks were observed in Fig. 2. Therefore, the change of the lattice constant due to dehydroxylation reaction represented by eq. (1) could be too small to detect.

$$2\mathrm{OH^-} = \mathrm{O^{2-}} + \mathrm{V} + \mathrm{H_2O}, \qquad (1)$$

where V represents the vacancy of $\mathrm{OH^-}$ site in the HAp structure.

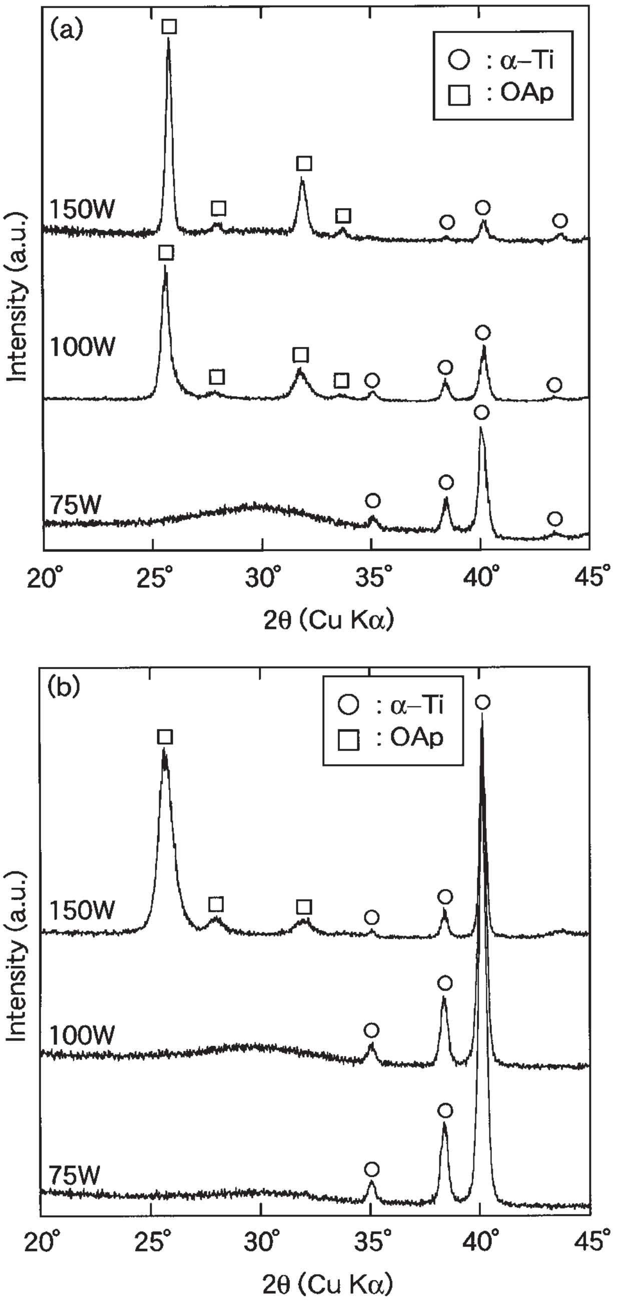

Fig. 4 XRD patterns of films prepared at total pressures of (a) 0.5 Pa and (b) 5 Pa. ($C_{\mathrm{O_2}} = 0\%$, deposition time = 18 ks)

Table 2 Values of Ca/P molar ratio in the films prepared at $C_{\mathrm{O_2}} = 0\%$ and total pressure of 0.5 Pa for the deposition time of 18 ks.

Method	RF power		
	75 W	100 W	150 W
FXS	1.81	1.76	1.65
ICP-AES	1.65	1.81	1.57

Figures 4(a) and (b) show α-2θ XRD patterns of the films prepared at the total pressures of 0.5 and 5 Pa, respectively, for the deposition time of 18 ks. ($C_{\mathrm{O_2}}$: 0%). In addition to the reflections of the OAp phase, the broad peak at around 30° was observed at lower RF powers. The broad peak could exhibit the formation of amorphous calcium phosphate (ACP) phase. Table 2 summarizes the values of Ca/P molar ratio in the films prepared at $C_{\mathrm{O_2}}$ of 0% and the total pressure of 0.5 Pa. The Ca/P values were close to that of OAp (1.67) and higher than that of the target material, β-TCP, (1.5). Lower mass atoms should be more scattered by plasma than atoms with higher mass atoms.[50] Therefore, it might be understood that the films of Ca/P molar ratio higher than that of the target were obtained. The RF power dependence of Ca/P molar ratio was different between the results obtained

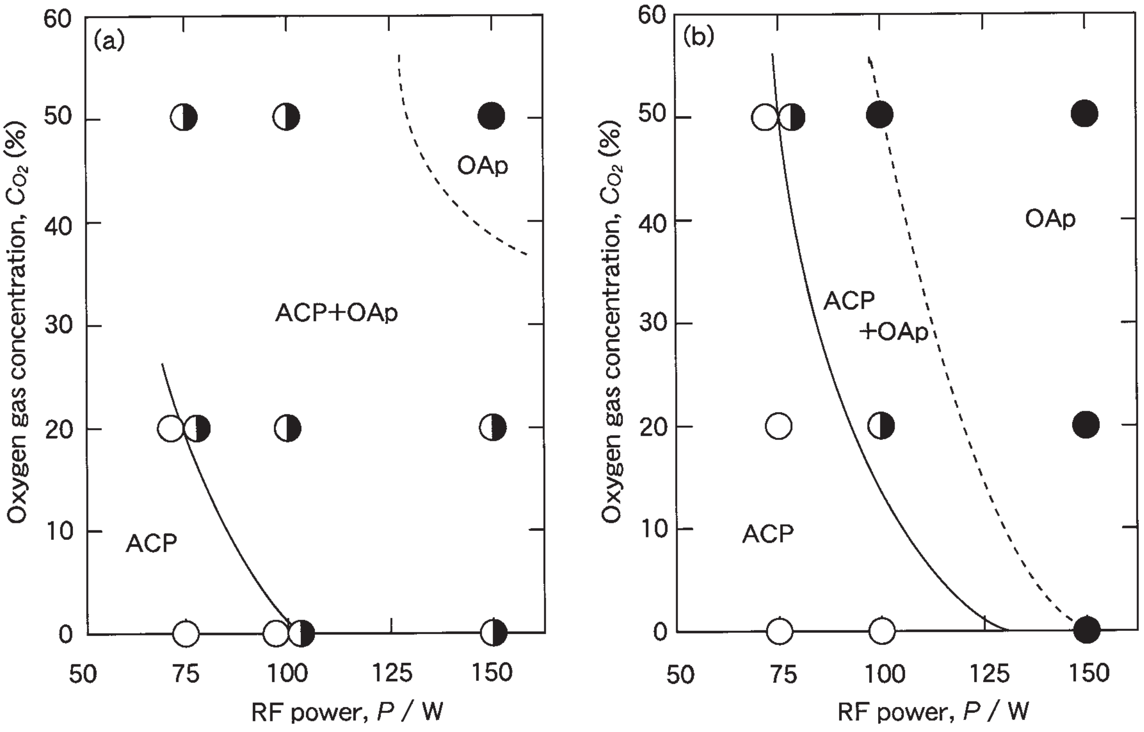

Fig. 5 Effect of oxygen gas concentration in the sputtering gas (C_{O_2}) and RF power on the phase in films at total pressures of (a) 0.5 Pa and (b) 5 Pa. (deposition time = 18 ks)

by FXS and ICP-AES measurements as shown in Table 2. Interactions of Ca with titanium substrates at the initial stage of the deposition might relate to the difference.

Figure 5 demonstrates the effects of C_{O_2} and RF power on the phase of films prepared for the deposition time of 18 ks. The films obtained in the present work consisted of OAp and ACP depending on C_{O_2} and RF power. It is understood that the kinetic energy of sputtered atoms or clusters would transformed into the energy for crystallization in RF magnetron sputtering.[50] The kinetic energy of argon ions could increase with increasing RF power and C_{O_2} at a specific RF power[49] and with decreasing total pressure.[33] The increase in kinetic energy of argon ions would cause the increase in kinetic energy for sputtering the target, and then the atoms or clusters could arrive at the substrate with higher kinetic energy accelerating the crystallization.

3.3 Preferential orientation

Figure 6 shows the θ–2θ XRD patterns of the films prepared at the RF power of 150 W and the total pressure of 5 Pa for the deposition time of 18 ks. The intensity of (002) peak ($2\theta = 25.9°$) increased with decreasing C_{O_2}. The preferred orientation of a specific ($h'k'l'$) plane for the OAp phase in the films was evaluated by Lotgering factor $F(h'k'l')$ as given by eqs. (2) and (3).[59]

$$F(h'k'l') = \frac{P - P_0}{1 - P_0} \tag{2}$$

$$P = \frac{\sum I(h'k'l')}{\sum I(hkl)}, \tag{3}$$

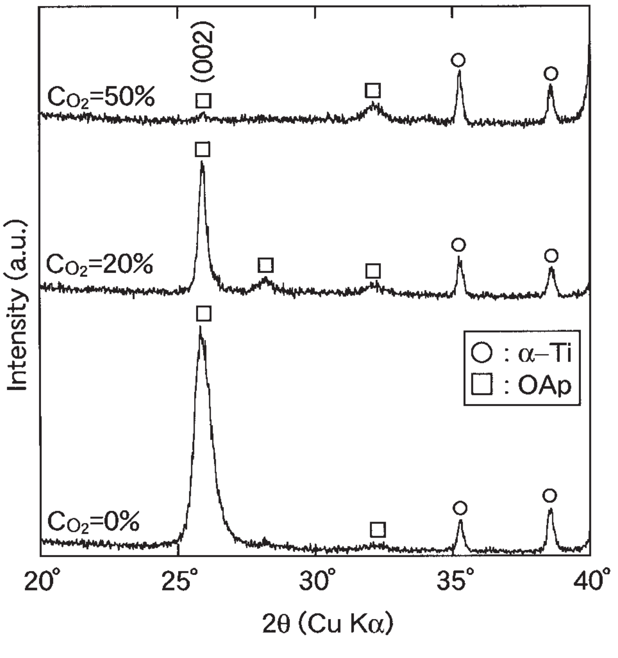

Fig. 6 XRD patterns of films prepared at total pressure of 5 Pa and RF power of 150 W for the deposition time of 18 ks.

where $I(hkl)$, $I(h'k'l')$, P and P_0 are the diffraction intensity of (hkl) plane, that of oriented ($h'k'l'$) plane, the ratio of intensity summation for the experimental data and that of JCPDS data, respectively. $F = 1$ and $F = 0$ mean perfectly oriented and non-oriented faces, respectively. Figure 7 shows the values of $F(002)$ of the OAp prepared at the RF power of 150 W, which were calculated by using the diffraction intensity of XRD patterns in the 2θ range between 20° and 45°. The values of $F(002)$ decreased with increasing C_{O_2} at the total pressure of 5 Pa, while $F(002)$ was almost independent of C_{O_2}, almost unity, at the total pressure of 0.5 Pa. It is well

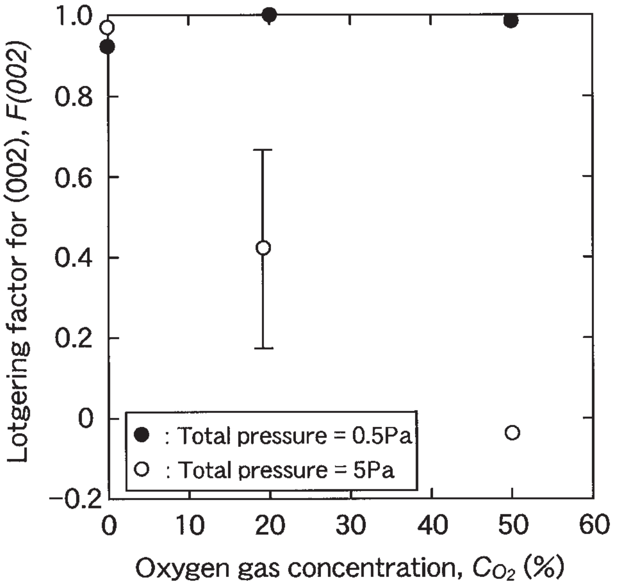

Fig. 7 Effect of oxygen gas concentration in the sputtering gas (C_{O_2}) on the Lotgering factor for (002) of OAp in the films prepared at RF power of 150 W.

known that HAp exhibits the anisotropy of reactivity with human saliva[60] and mechanical properties.[61,62] Therefore, the preferred orientation of OAp films should be controlled for the biomedical applications. Several researchers studied the preferred orientation in calcium phosphate films on Ti substrates by sputtering.[23,36,50] Although the (002) preferred orientation was mentioned in literatures, the relationship between the preferred orientation and the deposition conditions in RF magnetron sputtering has not been reported so far. The present work revealed that significantly (002) oriented OAp films can be obtained at lower total pressure and C_{O_2} conditions.

3.4 Deposition rate

Figures 8(a) and (b) represent the effect of RF power on the deposition rate of films at the total pressures of 0.5 and 5 Pa, respectively, for the deposition time of 18 ks. The deposition rate increased with increasing RF power. The time dependence of the deposition rate was shown in Fig. 9 at C_{O_2} of 0%, RF power of 100 W and total pressure of 0.5 Pa. The deposition rate became constant after about 3.6 ks. The effect of total pressure on the deposition rate is shown in Fig. 10. The deposition rate showed maxima at the total pressure of 1 Pa at C_{O_2} of both 0 and 20%. The highest deposition rate in the present work was 0.143 $\mathrm{nm \cdot s^{-1}}$ (0.515 $\mathrm{\mu m \cdot h^{-1}}$).

The increase in deposition rate of calcium phosphates using RF magnetron sputtering has been reported in the range of total pressures between 0.26 and 2.6 Pa by van Dijk *et al.*[33] The number of the argon ions increases with increasing total pressure. Then, they concluded that the deposition rate could be increased by the increase in sputtering yield. On the other hand, they also mentioned that the deposition rate would saturate or decrease at further higher pressures due to collisions of argon atoms before arriving at the substrate.[33] The trend of Fig. 10 could be in agreement with the explanation by van Dijk *et al.*[33]

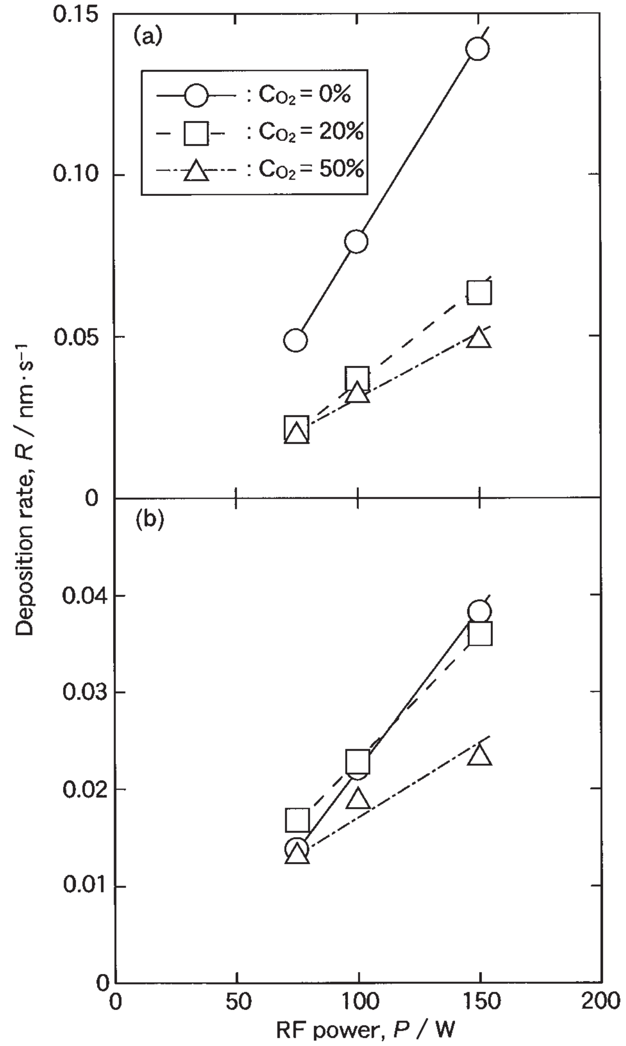

Fig. 8 Effect of RF power on deposition rate at total pressures of (a) 0.5 Pa and (b) 5 Pa for the deposition time of 18 ks.

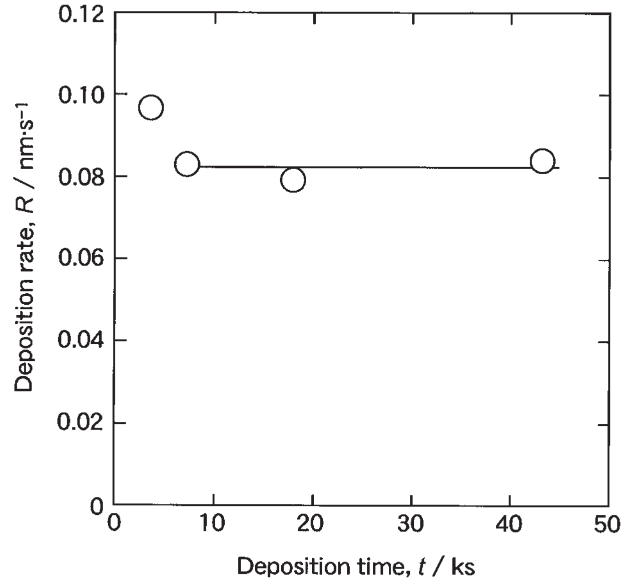

Fig. 9 Effect of deposition time on deposition rate of films at C_{O_2} of 0%, RF power of 100 W and total pressure of 0.5 Pa.

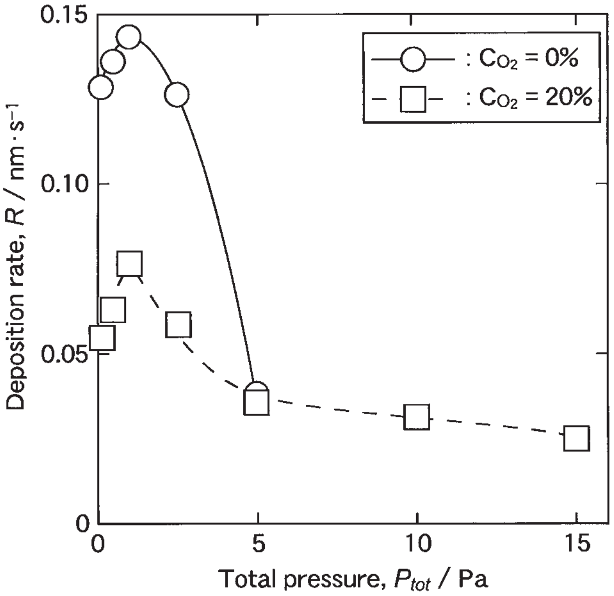

Fig. 10 Effect of total pressure on deposition rate of films at RF power of 150 W.

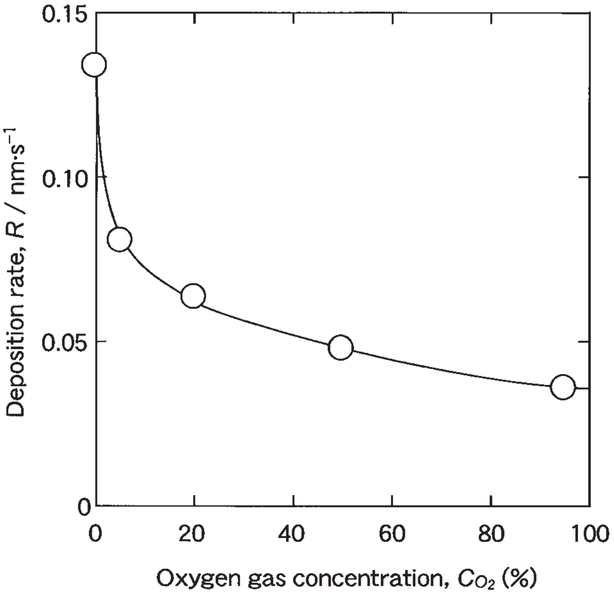

Fig. 11 Effect of oxygen gas concentration in sputtering gas (C_{O_2}) on deposition rate of films at total pressure of 0.5 Pa and RF power of 150 W.

Figure 11 shows the C_{O_2} dependence on the deposition rate of films. The deposition rate decreased sharply with increasing C_{O_2}. It was reported that the deposition rate decreased drastically by adding 1% O_2 to the sputtering gas.[49] It is known that high energy electrons also contribute the deposition in RF magnetron sputtering. Since O_2 would catch electrons to ionize O atoms as called "electron scavenger", the increase in C_{O_2} causes the decrease in deposition rates as demonstrated in Fig. 11.

4. Conclusions

Calcium phosphate films were prepared on commercially pure Ti substrates by RF magnetron sputtering using hot-pressed β-TCP targets. The following results were obtained.

(1) High density (>99.6%) β-TCP targets should be used to avoid the composition change of the target during RF magnetron sputtering.
(2) The films consisted of amorphous calcium phosphate and/or OAp phases. The OAp phase was detected in the conditions at higher RF powers and C_{O_2} and lower total pressures.
(3) The (002) preferred orientation of OAp was significant at lower total pressures and C_{O_2}.
(4) The deposition rate increased with increasing RF power and decreasing C_{O_2}, showing maxima at the total pressure of 1 Pa. The highest deposition rate was 0.143 nm·s^{-1} (0.515 µm·h^{-1}).

Acknowledgments

This research was supported by Special Coordination Funds for Promoting Science and Technology and a Grant-in-Aid for Scientific Research, under Contract No. 17656221 from the Ministry of Education, Culture, Sports, Science and Technology, Japan. This work was carried out under the cooperate research program of Institute for Materials Research, Tohoku University.

REFERENCES

1) W. G. Billotte: *"Ceramic Biomaterials," in The Biomedical Engineering Handbook*, 2nd Edition, ed. by J. D. Bronzino, Washington, D. C., (CRC Press, 2000) pp. 38-1–38-33.
2) G. Daculsi, O. Laboux, O. Malard and P. Weiss: J. Mater. Sci.: Mater. Med. **14** (2003) 195–200.
3) O. Gauthier, J. M. Bouler, E. Aguado, P. Pilet and G. Daculsi: Biomaterials **19** (1998) 133–139.
4) R. Fujita, A. Yokoyama, Y. Nodasaka, T. Kohgo and T. Kawasaki: Tissue and Cell **35** (2003) 427–440.
5) R. Fujita, A. Yokoyama, T. Kawasaki and T. Kohgo: J. Oral. Maxillofac. Surg. **61** (2003) 1045–1053.
6) H. Irie: Bull. Ceram. Soc. Jpn. **38** (2003) 55–57.
7) H. K. Koerten and J. van der Meulen: J. Biomed. Mater. Res. **44** (1999) 78–86.
8) S. Raynaud, E. Champion, J. P. Lafon and D. Bernache-Assollant: Biomaterials **23** (2002) 1081–1089.
9) N. Eidelman, L. C. Chow and W. E. Brown: Calcif. Tissue Int. **40** (1987) 71–78.
10) J. F. Osborn and H. Newesely: Biomaterials **1** (1980) 108–111.
11) Y. Yang, K. H. Kim and J. L. Ong: Biomaterials **26** (2005) 327–337.
12) M. Lind, S. Overgaard, C. Bünger and K. Søballe: Biomaterials **20** (1999) 803–808.
13) M. Tanzer, S. Kantor, L. Rosenthall and J. D. Bobyn: J. Arthroplasty **16** (2001) 552–558.
14) T. Jinno, D. T. Davy and V. M. Goldberg: J. Arthroplasty **17** (2002) 902–909.
15) M. T. Carayon and J. L. Lacout: J. Solid State Chem. **172** (2003) 339–350.
16) H. Ji, C. B. Ponton and P. M. Marquis: J. Mater. Sci.: Mater. Med. **3** (1992) 283–287.
17) E. Goyenvalle, N. J. M. Guyen, E. Aguado and N. Passuti: J. Mater. Sci.: Mater. Med. **14** (2003) 219–227.
18) J. Thanner, J. Kärrholm, P. Herberts and M. Malchau: J. Arthroplasty **15** (2000) 405–412.
19) K. A. Gross and C. C. Berndt: J. Biomd. Mater. Res. **39** (1998) 580–587.
20) C. F. Feng, K. A. Khor, E. J. Liu and P. Cheang: Scr. Mater. **42** (2000) 103–109.
21) P. Cheang, K. A. Khor, L. L. Teoh and S. C. Tam: Biomaterials **17**

(1996) 1901–1904.
22) I. Baltag, K. Watanabe, H. Kusakari, N. Taguchi, O. Miyakawa, M. Kobayashi and N. Ito: J. Biomed. Mater. Res. **53** (2000) 76–85.
23) J. C. G. Wolke, K. van Dijk, H. G. Schaeken, K. de Groot and J. A. Jansen: J. Biomed. Mater. Res. **28** (1994) 1477–1484.
24) L. Cleries, J. M. Fernándes-Pradas, G. Sardin and J. L. Morenza: Biomaterials **19** (1998) 1483–1487.
25) J. M. Fernandez-Pradas, L. Cleries, G. Sardin and J. L. Morenza: Biomaterials **23** (2002) 1989–1994.
26) F. Garcá, J. L. Arias, B. Mayor, J. Pou, I. Rehman, J. Knowles, S. Best, B. León, M. Pérez-Amor and W. Bonfield: J. Biomed. Mater. Res. **43** (1998) 69–76.
27) J. L. Arias, F. J. Garcá-Sanz, M. B. Mayor, S. Chiussi, J. Pou, B. León and M. Pérez-Amor: Biomaterials **19** (1998) 883–888.
28) B. Mayor, J. Arias, S. Chiussi, F. Garcia, J. Pou, B. León Fong and M. Pérez-Amor: Thin Solid Films **317** (1998) 363–366.
29) H. Zeng, W. R. Lacefield and S. Mirov: J. Biomed. Mater. Res. **50** (2000) 248–258.
30) Z. C. Luo, F. Z. Cui and W. Z. Li: J. Biomed. Mater. Res. **46** (1998) 80–86.
31) I. S. Lee, C. N. Whang, H. E. Kim, J. C. Park, J. H. Song and S. R. Kim: Mater. Sci. Eng. C **22** (2002) 15–20.
32) M. Hamdi and A. Ide-Ektessabi: Surf. Coat. Technol. **163–164** (2003) 362–367.
33) K. van Dijk, H. G. Schaeken, C. H. M. Marée, J. Verhoeven, J. C. G. Wolke, F. H. P. M. Habraken and J. A. Jansen: Surf. Coat. Technol. **76–77** (1995) 206–210.
34) K. van Dijk, H. G. Schaeken and J. A. Jansen: Biomaterials **17** (1996) 405–410.
35) K. van Dijk, V. Gupta, A. K. Yu and J. A. Jansen: J. Biomed. Mater. Res. **41** (1998) 624–632.
36) J. G. C. Wolke, J. P. C. M. van der Waerden, K. de Groot and J. A. Jansen: Biomaterials **18** (1997) 483–488.
37) J. G. C. Wolke, K. de Groot and J. A. Jansen: J. Biomed. Mater. Res. **43** (1998) 270–276.
38) J. G. C. Wolke, J. P. C. M. van der Waerden, H. G. Schaeken and J. A. Jansen: Biomaterials **24** (2003) 2623–2629.
39) K. Yamashita, M. Matsuda, T. Arashi and T. Umegaki: Biomaterials **19** (1998) 1239–1244.
40) M. Yoshinari, T. Hayakawa, J. G. C. Wolke, K. Nemoto and J. A. Jansen: J. Biomed. Mater. Res. **37** (1997) 60–67.
41) S. J. Ding, C. P. Ju and J. H. C. Lin: J. Biomed. Mater. Res. **47** (1999) 551–563.
42) J. L. Ong, K. Bessho, R. Cavin and D. L. Carnes: J. Biomed. Mater. Res. **59** (2001) 184–190.
43) K. Ozeki, T. Yuhta, Y. Fukui and H. Aoki: Surf. Coat. Technol. **160** (2002) 54–61.
44) Y. Yang, K. H. Kim, C. M. Agrawal and J. L. Ong: Biomaterials **24** (2003) 5131–5137.
45) A. Boyd, M. Akay and B. M. Meenan: Surf. Interface Anal. **35** (2003) 188–198.
46) L. Verestiuc, M. Morosanu, M. Bercu, I. Pasuk and I. N. Mihailescu: J. Crystal Growth **264** (2004) 483–491.
47) W. J. Lo, D. M. Grant, M. D. Ball, B. S. Welsh, S. M. Howdle, E. N. Antonov, V. N. Bagratashvili and V. K. Popov: J. Biomed. Mater. Res. **50** (2000) 536–545.
48) V. Nelea, C. Morosanu, M. Iliescu and I. N. Mihailescu: Appl. Surf. Sci. **228** (2004) 346–356.
49) K. Van Dijk, J. Verhoeven, C. H. M. Marée, F. H. P. M. Habraken and J. A. Jansen: Thin Solid Films **304** (1997) 191–195.
50) K. Van Dijk, H. G. Schaeken, J. C. G. Wolke, C. H. M. Marée, F. H. P. M. Habraken, J. Verhoeven and J. A. Jansen: J. Biomed. Mater. Res. **29** (1995) 269–276.
51) J. L. Ong, L. C. Lucas, W. R. Lacefield and E. D. Rigney: Biomaterials **13** (1992) 249–254.
52) H. Zeng, W. R. Lacefield and S. Mirov: J. Biomed. Mater. Res. **50** (2000) 248–258.
53) T. Kijima and M. Tsutsumi: J. Am. Ceram. Soc. **62** (1979) 455–460.
54) G. R. Fischer, P. Bardhan and J. E. Geiger: J. Mater. Sci. Lett. **2** (1983) 577–578.
55) J. Zhou, X. Zhang, J. Chen, S. Zeng and K. De Groot: J. Mater. Sci.: Mater. Med. **4** (1993) 83–85.
56) P. E. Wang and T. K. Chaki: J. Mater. Sci.: Mater. Med. **4** (1993) 150–158.
57) K. A. Gross, C. C. Berndt, P. Stephens and R. Dinnebier: J. Mater. Sci. **33** (1998) 3985–3991.
58) K. A. Gross, V. Gross and C. C. Berndt: J. Am. Ceram. Soc. **81** (1998) 106–112.
59) F. K. Lotgering: J. Inorg. Nucl. Chem. **9** (1959) 113–123.
60) H. Aoki: J. Surf. Sci. Soc. Jpn. **10** (1989) 96–101.
61) T. P. Hoepfner and E. D. Case: Mater. Lett. **58** (2004) 489–492.
62) T. Nakano, K. Kaibara, Y. Tabata, N. Nagata, S. Enomoto, E. Marukawa and Y. Umakoshi: Bone **31** (2002) 479–487.